Ecosystems (2025) 28:20
https://doi.org/10.1007/s10021-025-00966-9

ORIGINAL ARTICLE

ENSO Wildfires Impact Amazonian Floodplains in Complex Ways

Peter van der Sleen,[1]* Mathieu Decuyper,[1] Bernardo M. Flores,[2] J. Ethan Householder,[3] and Milena Holmgren[1]

[1]*Environmental Sciences Department, Wageningen University, Droevendaalsesteeg 3a, 6708 PB Wageningen, The Netherlands;* [2]*Graduate Program in Ecology, Federal University of Santa Catarina, Florianópolis, SC 88040-900, Brazil;* [3]*Wetland Ecology, Institute for Geography and Geoecology, Karlsruhe Institute for Technology, Karlsruhe, Germany*

Abstract

Amazonian floodplains are the most extensive and biodiverse riverine habitat on Earth. They currently face unprecedented fire regimes as climate change increases the frequency and intensity of drought. While it is clear that fire impacts on floodplain ecology can be severe, fire regimes and their effect on forest ecosystems have yet to be fully examined across the considerable spatial and ecological heterogeneity of Amazonian floodplains. We used the MODIS burned area product to map fire occurrence across Amazonian floodplain forests. Next, we assessed forest recovery after burning using NDVI values from LandSat images. We specifically focused on differences in wildfire dynamics and forest recovery after burning across floodplains associated with the three main river types in the Amazon basin (black-, clear-, and white-water rivers). We found that the occurrence of forest fires in floodplains is strongly associated with ENSO events and increases as land-use intensity increases, dry seasons get longer, soils become sandier, and the synchrony between flooding and precipitation patterns increases. Post-fire forest recovery is slower, and reburning risk is higher, on nutrient-poor floodplains of black-water rivers, compared to the nutrient-richer floodplains of white- and clear-water rivers. Moreover, forest recovery is significantly slower in regions flooded for prolonged periods, regardless of river type. Our results call for urgent prevention and monitoring of floodplain forest fires across the Amazon basin, with particular attention to black-water floodplains, to prevent large-scale vegetation shifts and cascading ecosystem changes on biodiversity and ecosystem services provided by floodplain forests.

Key words: Amazon fire regime; Floodplain forest; Forest recovery rate; Flooding; Resilience; River type.

Received 8 July 2024; accepted 2 February 2025;
published online 25 February 2025

Supplementary Information: The online version contains supplementary material available at https://doi.org/10.1007/s10021-025-00966-9.

Author Contributions: Peter van der Sleen and Milena Holmgren designed study. Peter van der Sleen and Mathieu Decuyper performed the analyses. All authors provided feedback that was critical for the development of the study. Peter van der Sleen wrote the first draft of the manuscript; all authors contributed to the writing of following manuscript drafts.

**Corresponding author; e-mail:* peter.vandersleen@wur.nl

Introduction

Floodplain forests extend across ~ 14% of the Amazon basin, and link terrestrial and aquatic biodiversity hotspots throughout the largest riverine system on Earth (Wittmann and others 2006; Householder and others 2024). These seasonally flooded environments regulate the hydrological cycle of northern South America (Gumbricht and others 2017) and store globally relevant carbon stocks. Fire has not, until recently, been considered an important disturbance in Amazonian floodplains where conditions are typically wet and unamenable to fire (but see Sanford and others 1985; Feldpausch and others 2022 for paleontological perspective). However, increasing drought conditions and associated wildfires have impacted even the wettest parts of the Amazon basin (Flores and others 2014; Flores and others 2017; Carvalho and others 2021). Wildfires in Amazonia, as in other tropical rainforests, are strongly associated to El Niño Southern Oscillation (ENSO) (Holmgren and others 2001; Alencar and others 2011), when conditions become sufficiently dry to facilitate fire ignition (Alencar and others 2015). Although the impact of these wildfires has received considerable attention (Barlow and Peres 2008; Malhi and others 2008; Cochrane and Barber 2009; Aragão and others 2018), most research has focused on non-floodplain or ''upland'' forests, that lie above the upper limit of seasonal river flooding. Yet, the risks and consequences of fire in floodplain forest are likely fundamentally different from non-floodplain forests (de Resende and others 2014; Almeida and others 2016; Flores and others 2017). Evidence suggests that floodplain forests across the Amazon are less resilient to drought conditions and fire, compared to upland forests, implying that they could be the first to collapse if drying conditions continue to increase (Flores and others 2017).

Generalizations on the risks and consequences of fire in Amazonian floodplains are, however, complicated by their heterogeneous nature, on both small spatial scales (for example, associated with topography and hence flooding duration) and larger spatial scales (for example, Amazonian subbasins and their geomorphologies). Across the Amazon basin, nutrient and sediment concentrations of rivers vary in important ways, and this may result in different fire risks and very different trajectories of floodplain forest regrowth after burning. For example, in nutrient poor black-water floodplains (mainly distributed in the north-eastern Amazon, but also along the tributaries of most subbasins; Figure 1a), forests typically have lower tree density and stature, with tree heights around 15–20 m (Junk and others 2015; Almeida and others 2016). Consequently, atmospheric drought conditions can lead to strong desiccation in the understory (de Resende and others 2014; Almeida and others 2016), which in combination with a thick root mat (dos Santos and Nelson 2013), increases fire risk (Flores and others 2016; Carvalho and others 2021). Because black-water rivers have an exceptionally low content of dissolved nutrients (Furch 1984), carrying few sediments (Latrubesse and Franzinelli 2005), nutrient loss after burning is not replenished by floodwaters and soils quickly lose fertility and become more sandy (Flores and Holmgren 2021a). Black-water floodplain forests may, therefore, regenerate very slowly after burning, and when exposed to repeated fires can transition to an open, white-sand savanna state (Flores and Holmgren 2021a).

In other parts of the basin however, such as the floodplains of white-water rivers, soils are annually inundated by clay- and nutrient-rich water (Goulding and others 2003; Junk and others 2012). Flooding, therefore, regularly replenishes clay minerals and nutrients; a mechanism that could potentially facilitate rapid forest regrowth after a disturbance. Floodplain forests of clear-water rivers (Figure 1a) may show intermediate forest resilience relative to black- and white-water floodplains.

The heterogeneity of floodplain forests has remained largely overlooked in the analysis of fire and its consequences in Amazonian floodplains. Here, we assess floodplain fire regimes and forest recovery after burning, examining these across a greater degree of geographic and environmental variation than hitherto considered. Within this heterogeneity, including multiple environmental and anthropogenic drivers across spatial scales, we expect a wide spectrum of floodplain fire regimes and responses that can provide a more complete view of floodplain fire regimes and forest resilience. Understanding these dynamics at a finer spatial scale can better inform research priorities and guide ecosystem management and conservation efforts in the face of increasing fire risk.

Methods

We performed two main analyses: (1) mapping of fire occurrence in floodplains across the Amazon basin, and relating fire occurrence to environmental conditions, and (2) assessing vegetation recovery after burning in the different floodplain forest types (Table 1).

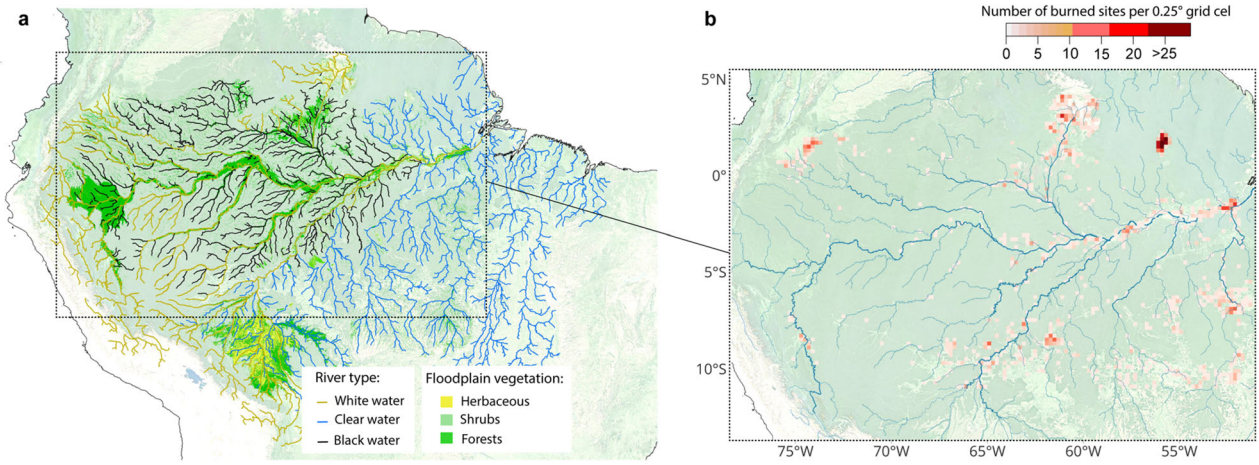

Figure 1. **a** Distribution of white, clear, and black-water rivers (based on data from Venticinque and others (2016)), and vegetation type covering central Amazonian floodplains (based on data from Hess and others (2015)). The dashed rectangle shows the study region. **b** Estimation of fire occurrence across Amazonian floodplains in the period 2000–2020. An individual burned site is an area of 0.5–6.25 km^2. Note that the scale bar does not translate to actual surface area burned, since the estimations are extrapolated from a random sample of 200,000 floodplain points of 2.5 × 2.5 km^2 each (10,000 sampling point per year).

Table 1. Overview of Variables, Data Sources, and Sampling Scales

Response variable	Fire occurrence and return frequency	Forest recovery	
Scale	**Basin**	**Basin**	**Local (within floodplains)**
Response variable data source	Modis Burned Area product	LandSat NDVI and Avocado Algorithm	
Sample size	200,000 points, 2.5 × 2.5 km^2 each	23 sites, 100 km^2 each	
Timespan	2001–2020	2005–2010	
Environmental (explanatory) variables:	River type, Dry season length, Land-use intensity, Soil texture, Flooding-precipitation synchrony	River type	Elevation
Resolution	0.1°	Pixels of 30 m across	

Data sources of explanatory variables can be found in the Methods section

Study Area

Floodplains in the Amazon were categorized into three main types: white-, clear-, and black-water river floodplains, using the results of Venticinque and others (2016) and the freshwater ecoregions of the world (Abell and others 2008) to define watershed boundaries (Figure 1a).

We focused our analyses on the Amazon basin north of 11°S for three main reasons. Firstly, different climatic teleconnections are associated with droughts (and fires) above and below ~ 11°S (Ortega Rodriguez and others 2023). North of ~ 11/12°S drought events are strongly associated with ENSO events, whereas in the southern part of the Amazon basin, a strong teleconnection to sea surface temperature variability in the tropical Atlantic Ocean also underlies drought and fire occurrence. Secondly, because of higher human population density and land-use change, fire occurrence is very high in the southern part of the Amazon basin (Alencar and others 2015) and this overrepresentation may bias our focus on differences in fire regimes across the main river types of the central Amazon basin. Thirdly, south of 11 degrees large regions are present that are dominated by more open, and naturally more fire-prone, vegetation types, such as the grasslands of the Llanos de Moxos in Bolivia and Cerrado savannas in Brazil. Including such areas would bias our results.

Mapping Fire Occurrence

We used monthly data of the MODIS Burned Area Product at a 500 m resolution (MCD64A1 Version 6; Giglio and others 2018) to detect forest fires and their potential drivers in Amazonian floodplains. We validated the ability of the MODIS Burned Area product algorithm to detect floodplain fires by comparing detection rates to 75 fire scars of known origin distributed across the basin (Flores and others 2017). We found that ~ 50% of the known burned areas were also found in the MODIS Burned Area product; most of the remaining fire scars were likely undetected because of their relatively small size. We also compared the known fire scars to fires detected by the MODIS Thermal Anomalies product (MOD14A2) but found a much lower detection rate. The latter result is possibly a consequence of the nature of forest fires in floodplains, being commonly ground fires that may be concealed in closed-canopy forests. However, such fires can ultimately lead to tree mortality rates of up to 90% (Flores and others 2014) and create burned areas that are detected in the MODIS Burned Area product. We hence choose the MODIS Burned Area product in the first part of our analyses. Although MODIS Burned Area captures most large forest fires, our estimation of fire occurrence is likely conservative given its relatively coarse resolution. We assume that undetected fires are not systematically biased with respect to the main river types investigated (that is, that (un)detention rates do not differ between the main river types). As such our conservative fire detection should not change observed differences between the river types and our environmental inferences.

Because floodplain forests cover a large area (~ 250,000 km^2), we used a sampling approach by which ~ 25% of this area was randomly assessed each year from 2001 to 2020. To this end, a total of 10,000 points of 2.5 × 2.5 km^2 were randomly taken for each year (note that each year a different set of random points was sampled). We used the wetland mask of Hess and others (2015) to select these 200,000 (= 10,000 points × 20 years) sample points in floodplains only. For each selected point, we recorded if a fire occurred in any of the months during the sample year, and how large the burned area was (that is, how many 500 × 500 m pixels burned). For all points for which a burned area was detected, we used the full MODIS burned area time series to assess: (1) if the area burned more than once during 2001–2020 and (2) the mean time it took to reburn. We used ANOVA to test for differences in burn frequency and mean reburn times between the three main floodplain forest types.

Environmental Data

To assess drivers of spatial and temporal fire occurrence, we used the following environmental data:

(1) Dry season length, defined as the number of months with mean monthly precipitation ≤ 100 mm per year (averaged over the period 1950–2020), and based on CRU TS4.05 precipitation data at 0.5° resolution (Jones and others 2012);
(2) Land-use intensity using the Global Human Modification of Terrestrial Systems data set, a cumulative measure of the human modification of terrestrial lands based on 13 anthropogenic stressors (including human density, mining and energy production, density of roads, percentage of cropland, and livestock density) and their estimated impacts for the median year of 2016, at a 1-km resolution (Kennedy and others 2020);
(3) Soil texture data (content of sand, in g/kg, at 15–30 cm soil depth) from ISRIC soil grids at a 250-m resolution (Poggio and others 2021).
(4) Flooding-precipitation synchrony; if droughts occur during floodplain inundation periods, forest fire risk could be strongly reduced. Thus, the synchrony between the period of low precipitation (dry season) and floodplain inundation could be an important determinant of floodplain fire occurrence. Floodplain inundation was estimated using GRACE Tellus satellite data at 1° resolution, which measures anomalies in the earth gravitational field that are indicative of the distribution of water across the planet (Landerer and Swenson 2012; Landerer 2021). Previous studies have shown that the annual hydrology of the Amazon basin is clearly captured by GRACE (Tapley and others 2004). Yet, to better estimate river level fluctuations for the floodplain pixels that are the focus of our study, we used the scaling coefficients provided by Landerer (2021) to remove the 300 km wide Gaussian filter that is standard applied to the data. We next used the GRACE Tellus data from 2002 to 2020 to calculate for each 1°×1° pixel an average yearly flood cycle at bimonthly intervals (the turnaround time of Grace). Flooding at every time interval is calculated as the mean over the 20-year period of Grace measurements (Figure S1). Using river level data from Manaus,

Brazil (Agência Nacional de Águas e Saneamento Básico; ANA), we found that GRACE Tellus data and observed river level fluctuations strongly coincided (Figure S1a). To correlate temporal flooding patterns with precipitation, we used CRU TS4.05 data to create a time series of mean monthly precipitation from 2002 to 2020 for every pixel, at the same temporal resolution of the GRACE data. Annual patterns in flooding (GRACE Tellus) and precipitation (CRU TS4.05) were correlated, with the correlation coefficient indicating the level of synchrony between rainfall and floodplain inundation: high positive correlation coefficients (high synchrony) would suggest that low precipitation seasons (dry season) coincide with low-water periods, while strong negative correlation (high asynchrony) would suggest that low precipitation seasons occur when floodplains are inundated (Figure S1b). We also used the mean annual patterns to determine the month of lowest precipitation (that is peak of the dry season) and the month of lowest river level. We next calculated the delay (in months) between the two, for each 1°×1° grid cell (Figure S1c).

(5) Lastly, ENSO3.4 based on the Hadley Centre Sea Surface Temperature dataset (HadISST) at 1° resolution (Rayner and others 2003) was used to assess the role of ENSO variability on temporal fire frequency in floodplains.

Prior to data analyses, the spatial resolution of the environmental datasets was converted to 0.1° resolution. Fire occurrence in each 0.1° grid cell was calculated as the total number of burned points detected in that 0.1° grid cell over the period 2001–2020. We thus do not estimate the actual surface area burned, since the estimations are extrapolated from fire occurrence in the random sample of 200,000 floodplain points of 2.5 × 2.5 km^2 each. Instead we estimate where fires were concentrated during the period 2001–2020. Inspection of scatterplots of fire occurrence and each of the environmental conditions justified the use of 'simple' linear models. Regression models were therefore used to assess the covariance between fire occurrence (in each 0.1° grid cell) and environmental conditions (in each 0.1° grid cell). Model selection was based on step-wise selection of environmental variable using AIC. Variance inflation factors (VIFs) were calculated to assess collinearity of predictor values; VIF-values were below 2 for all predictors. All analyses were performed in R; main packages used were MODISTools (Hufkens 2023) and Raster (Hijmans 2023).

Mapping Vegetation Recovery

We used the recently developed AVOCADO (Anomaly Vegetation Change Detection) algorithm (Decuyper and others 2022) to assess vegetation recovery on burned areas. The AVOCADO algorithm was used here to derive changes in the normalized difference vegetation index (NDVI) data from LandSat images relative to a predefined (undisturbed) reference forest within each site. We used NDVI instead of the normalized difference moisture index (NDMI), because the latter is likely unreliable in habitats that are flooded part of the year (due to its sensitivity to moisture), which will increase the probability of false recovery rates during the flooding season (DeVries and others 2015).

Specifically, the AVOCADO algorithm assesses: (1) the time a pixel's NDVI values consistently drop outside of the 95th percentile of NDVI values of a predefined (mature) reference forest (Figure S2), and (2) the time that pixel's NDVI values are consistently back at the level of the reference forest (Figure S2d). Note that the following analyses were thus based on the behavior in individual pixels instead of entire fire scars. Because AVOCADO uses all available LandSat images of a selected area when making a robust and accurate forest phenology baseline, it is labor intensive and computationally heavy. We therefore could not assess forest recovery in each of the 2.5 × 2.5 km^2 sample point that was flagged as burned by the MODIS Burned Area product. Instead, we selected 23 larger sites of 100 km^2 each, distributed in floodplain forests of black- (n = 8), clear- (n = 7), and white-water (n = 8) rivers (Figure S2). Site numbers were chosen considering sufficient replication across the basin and required computation time. Sites were selected based on the fire maps of the MODIS burned area product and hence concentrated in regions where fires occurred. We did not select sites located closely to large settlements or agricultural frontiers, to avoid confounding effects of land-use change. For each site, the avocado algorithm was used to quantify forest disturbance and recovery. More details on the method can be found in Decuyper and others (2022).

To assess forest recovery rates within and across the sites, we focused on burned areas formed in 2005. We choose 2005 because it is the first large-scale drought (and fire) year in the available time series (Marengo and others 2008). Forest recovery

rate was calculated as the time it took for the NDVI data to return to, or exceed the most probable forest reference baseline within the NDVI frequency distribution of the reference forest (Decuyper and others 2022).

AVOCADO detects a disturbance as a drop in NDVI. Such a drop can result from forest fires, but other disturbances can reduce NDVI as well. For example, white-water river channels are highly dynamic and river meandering erodes banks and forests. To avoid false disturbance detection by the AVOCADO algorithm, in case a forest pixel became a ''water'' pixel in subsequent LandSat images, we carefully masked out all open waterbodies in the LandSat images. To this end, we used the semi-automatic classification plugin (SCP) in QGIS (Congedo 2021). For each sampling site, we selected a recent, cloud-free, LandSat image during the low-water season. Next, the SCP was used to classify pixels into five categories: water, grass, shrubs, low-floodplain forest, and high floodplain forest. All avocado results from pixels classified as ''water'' were removed from subsequent analyses. The AVOCADO method also limits false detection due to temporal flooding, because at least three consecutive pixels need to be below the 95% CI (disturbance) or reach the line of the highest frequency of observed NDVI values (dark red line in Figure 3d) in case of regrowth. Furthermore, a ''water'' pixel will result in NDVI values between 0 and −1, which is different from NDVI changes due to forest loss, when values typically drop to around 0.2 (Figure S2). Riverbank erosion and seasonal flooding effects are, therefore, unlikely to be detected as a forest disturbance event. We tested for differences in forest recovery (that is, mean forest recovery rate and the mean percentage of burned pixels not recovered in each of 23 study sites) between the main floodplain forest types using ANOVA.

Habitat Heterogeneity in Floodplains

Floodplain tree species differ in their ability to tolerate prolonged flooding, and within each of the major floodplain forest types, the composition and structure of the forest therefore changes along the flooding gradient, that is with distance from the main river channel (Householder and others 2024). To assess the role of such habitat heterogeneity on recovery rates, we used high-resolution elevation data, since low elevation areas will experience the longest flooding duration, while higher elevation sites are only flooded shortly each year or only in years with exceptional flooding height. The Global Multi-resolution Terrain Elevation Data (GMTED2010) was used to obtain elevation data at 7.5-arc-second (225 m) spatial resolution (Danielson and Gesch 2011) for each 100 km^2 sample site. Elevation was standardized to allow for intersite comparisons by subtracting the minimum site elevation (assumed to represent river water level) from all other elevations. Hence, our standardized elevations are supposed to represent elevation above river water levels. Mixed-effect models were used to assess relationships between forest recovery and elevation, as these can account for the nested structure of the data by including each 100 km^2 site as random variable.

Results

Fire Occurrence

Fire is a widespread disturbance across the Amazon basin (Figure 1b), but its occurrence significantly increases with land-use intensity, dry season length, flood-precipitation synchrony, and the proportion of sand in the soil (Table S1, Figure S3). The annual burned area fluctuates substantially among the three floodplain types, but averages across years are quite similar regardless of floodplain type (Figure 2a). This however, does not mean similar fire risk among floodplain, due to the differences in floodplain extents: the area that burns annually is proportionally larger clear-water (0.67%) and black-water (0.47%) floodplains compared to white-water (0.20%) floodplains (Figure 2a). Temporal variability in fire occurrence in Amazonian floodplains is significantly correlated to sea surface temperature variability in the tropical Pacific (that is, ENSO3.4 variability; Figure 2b). We found no significant trends in the number of pixels that burned, or their total area, from 2001 to 2020 in any of the three river types (Figure 2a).

Risk of Reburning

Of the 200,000 random sites assessed, 1837 sites were flagged as burned. Using the full MODIS Burned Area time series for these 1837 burned sites, we found that the proportion of burned sites (that is, pixels) that reburned at least once during the period 2001–2020, was significantly higher in black-water floodplain forests compared to white- and clear-water floodplain forests (Figure 3b; ANOVA df = 1, F-value = 184, p-value < 0.0001). On average reburning risk was 62–73% higher in the black-water floodplains (mean: 76%) compared to white-water floodplains (mean: 47%) and clear-water floodplains (mean: 44%). We also found that

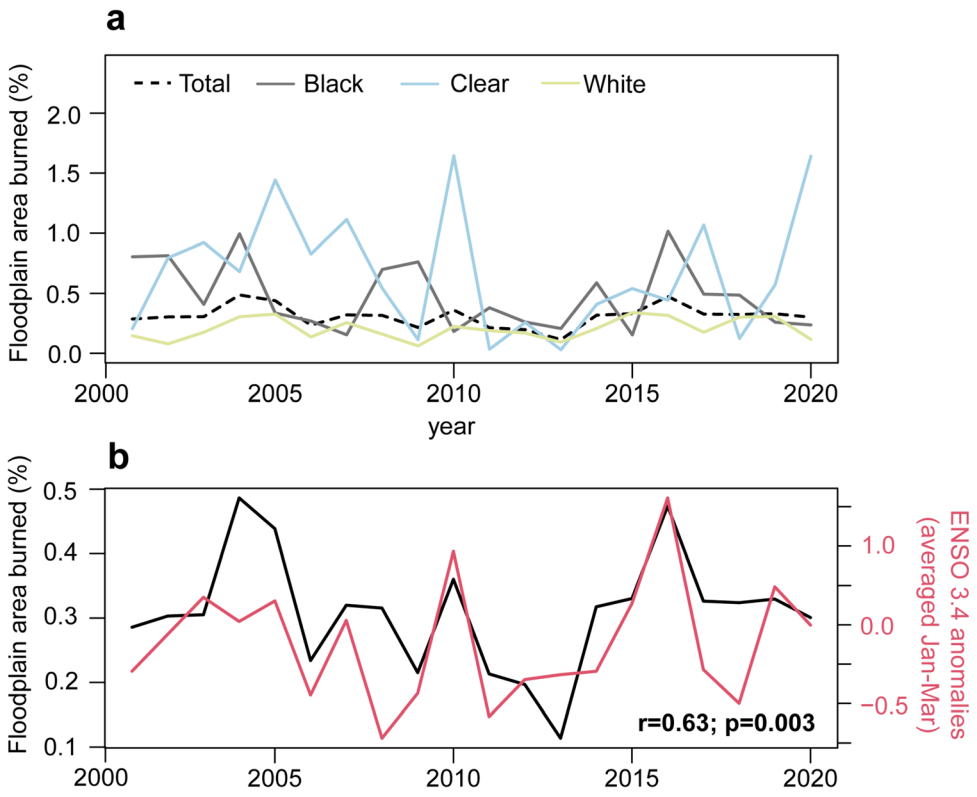

Figure 2. **a** Floodplain area that burned annually from 2001 to 2020 for each of the three main river types, as well as across the entire basin (total; same as shown in panel b). Spatial division of river types in Figure S5a. Percentage calculated as the total area that was detected in each year as burned, divided by the total surface area surveyed for each river type (62.500 km^2/year in total). **b** Total floodplain area burned annually from 2001 to 2020 (as a percentage of the total; black line) covaries with El Niño-Southern Oscillation (ENSO 3.4 index averaged for the months January to March; red line). Pearson's correlation coefficient and associated p-value are given in panel b.

the minimum time between fire events was significantly shorter in black-water floodplain forests compared white- and clear-water floodplain forests (Figure 3b; ANOVA, df = 1, *F*-value = 95, *p*-value < 0.0001). On average the time for a pixel to be detected as reburned was 60% shorter in black-water floodplains (mean: 3.2 years) than in clear-water floodplains (mean: 4.1 years) and white-water floodplains (mean: 5 years).

NDVI Recovery After Burning

We found that NDVI recovery after burning is significantly slower in black-water floodplains compared to white- and clear-water floodplains (ANOVA df = 2, *F*-value = 11.5, *p* = 0.0003; Figure 3b). On average, the NDVI recovery time was 20% and 35% slower in black-water floodplains forests compared to white- and clear-water floodplain forests, respectively. In addition, the percentage of pixels that burned in 2005 and that did not recover after 15 years was significantly higher in black-water floodplains (mean = 49%) than in clear-water (mean = 18%) and white-water floodplains (mean = 27%; ANOVA df = 2, *F*-value = 6.9, *p* = 0.004; Figure 3b). We also found that within floodplains, fire occurrence and post-fire forest recovery time were significantly higher in low elevation areas. This result was consistent across all river types (Figure S4, Table S2).

Discussion

We found that fire occurrence is widespread in the Amazon floodplains but is concentrated in the eastern part of the basin. Temporal variation in the frequency of floodplain forest fires was significantly related to ENSO (Figure 2b), corroborating results from previous studies focusing on Amazonian droughts and fires in the general (for example, Fonseca and others 2017; Aragão and others 2018; Berenguer and others 2021; dos Reis and others 2021). The spatial occurrence of forest fires on the other hand was significantly related to land-use intensity, soil texture, dry season length, and the

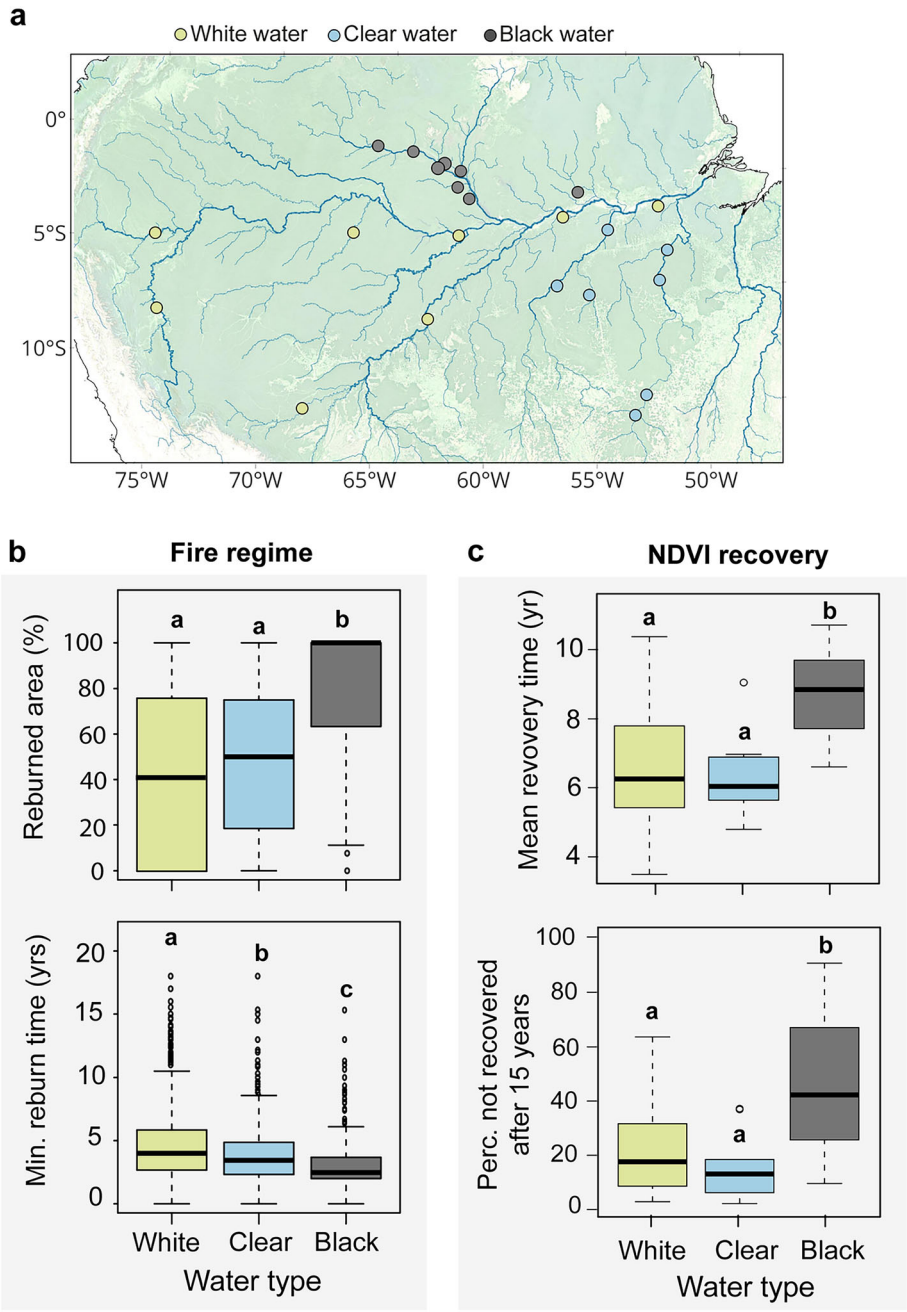

Figure 3. **a** Distribution of the 23 study sites, each 100 km^2, underlying the results shown in panel c. Note that the assignment of floodplain sites to white-, clear-, or black-water rivers is based on the water type of the main tributary river in each of the sub-basins, but smaller tributaries may have a different water type (Figure 1a). **b** The proportion of areas that burned at least twice during the period 2001–2020 and the mean minimum time to reburn across the three main river types. **c** Mean NDVI recovery time and the percentage of burned areas that did not recover after 15 years across the three main river types. Small letters in panels b and c indicate significant differences between floodplain forests in different river types.

synchrony between flooding and precipitation (Figure 1, S2, Table S1). Some of these factors are well-known drivers of increased forest fire risk (Flores and others 2017; Silveira and others 2020), but our results highlight the additional roles of soil texture and the interaction between flooding and precipitation patterns for floodplain forests. Soil texture affects many forest properties that in turn influence fire risk, as well as forest recovery after burning, which is further discussed below. Regions

were flooding and precipitation cycles are, on average, highly synchronous appear to be more prone to burn (that is, where precipitation dry seasons generally coincide with periods of low river levels). Likewise, drought-induced forest fires appear less likely to occur when floodplains are inundated (high asynchrony), allowing forests to escape from fire, even when they are exposed to climatological droughts. However, we do acknowledge that the coarseness of the data used to calculate flooding cycles may have led to high inaccuracies (Figure S1) and that the precise role of flood-precipitation synchrony warrants further study.

Overall, the environmental variables explained only 3% of the fire occurrence from 2001 to 2020, which likely reflects the scattered nature of forest fires, the role of microenvironmental conditions, as well as the relatively short time period analyzed. In addition, spatial variability of climate extreme events (for example, exceptional droughts or flooding) was not explicitly considered in our test of the potential drivers of fire, while this has strongly affected fire occurrence during the last decades (Aragão and others 2007; Gloor and others 2013; Barichivich and others 2018; Silveira and others 2020).

Impact of Fire

The consequences of fire varied between floodplain types, with forests on black-water floodplains showing the slowest recovery rates compared to forests on white- and clear-water floodplains (Figure 3). Slow recovery of black-water floodplain forests after disturbances has been related to the higher proportion of sand and low nutrient content in the topsoil (Figure S3, S5), causing lower growth rates compared to forests in the other major floodplain types (Schöngart and others 2005; Junk and others 2015; Flores and others 2016; Flores and others 2017; Carvalho and others 2021). Experimental evidence indicates that slow recovery of black-water forests after fire can also be related to seed dispersal limitation (Flores and Holmgren 2021b), for instance due to changes in the composition of aquatic- (Lugo Carvajal and others 2023) and terrestrial animal communities (Ritter and others 2012) observed in burned black-water forests. Black-water floodplain forest may therefore need decades to recover dense canopies that exclude grasses and reduce flammability (Flores and others 2016) and centuries to recover to a late-successional forest state (Junk and others 2015). Consequently, black-water floodplains remain in a prolonged early successional stage after burning, characterized by dense herbaceous vegetation and a low density of young trees and shrubs (Flores and others 2016). Such open vegetation can dry out easily when drought conditions prevail (for example, during El Niño events; Figure 2), increasing the risk of reburning. Indeed, we found that the percentage of areas that reburned at least once over the period 2001–2020 was significantly higher in black-water floodplains compared to clear- and white-water floodplains. Our study thus provides evidence that repeated fires are driving a vegetation transition in black-water floodplain forests from closed-canopy forests to open vegetation types. Such fire traps determine vegetation transitions in upland regions (for example, Hoffmann and others 2009; Oliveras and Malhi 2016) and here we show that fire traps can also lead to state transitions in one of the wettest regions of the world. Higher clay content and nutrient status, and higher abundance of animal dispersers, in clear- and white-water floodplains on the other hand, promotes fast forest recovery after burning, lowering the risk of recurrent burning.

Within floodplains forests, independent of the river type, recovery time increases at lower elevation. The extended flooding period at low topographies decreases the length of the tree growing season (that is, the dry season) and as a consequence lowers forest recovery rates (Resende and others 2020). Low elevation sites also exhibit the most specialized tree communities, including many endemic species adapted to periods of flooding lasting > 9 months (Junk and others 2015). Increasing fire perturbations could, therefore, impact the abundance of such highly-adapted and often slow-growing species, such as the iconic *Eschweilera tenuifolia* that may live up to 1000 years (Resende and others 2020).

Limitations

Our estimations of forest recovery are likely very conservative since we used the recovery of the NDVI signal for a forest. Field observations indicate that some fire scars in black-water floodplains can be colonized relatively quickly by herbaceous vegetation (Flores and others 2016), reaching high density and heights higher than 2 m. The leaf area index of such vegetation cover may resemble NDVI values of a reference forest site. Hence, the reported forest recovery rates here are likely a considerable overestimation of actual forest recovery rates. Therefore, it is particularly noteworthy to realize that although NDVI may overestimate recovery

rates, on average 49% of the burned pixels in black-water floodplains, did not recover after 15 years (Figure 3b), while this percentage was 18% and 27% in clear- and white-water floodplain forests. It is unlikely that such a lack of forest recovery in black-water floodplain forests (or in any of the other river types) was a consequence of land-use change, for example of forest clearing for agricultural purposes. Our sampling sites were carefully selected to avoid this issue and images were manually checked to confirm land-use change was absent, which can easily be identified on remote sensing images by rectangular or straight-lined disturbances, instead of more erratic disturbance shapes.

Floodplains are highly heterogeneous habitats (Junk and others 2011) and the use of only three main floodplain forest types is, therefore, an over-simplification of a complex reality. This is especially true for white-water floodplains that cover the greatest area across the Amazon, and in our rough division (Figure S5) include many black-water tributaries (Figure 1a). This implies that the range of possible responses of white-water forests to fire could be broader than we actually found. Furthermore, even within true white-water floodplains, burning risk and recovery after burning may vary spatially due to differences in climatic conditions (with mean annual precipitation varying between < 1000 and over 4000 mm within the area covered by white-water floodplain forests), soil properties (Figure S5), and/or flooding regimes (for example, Goulding and others 2003).

Future Directions

Floodplain ecosystems form a continuous network that spreads across the core of the Amazon forest. Increased floodplain fires and forest mortality within this core could affect the resilience of the system at larger scales, which is particularly the case in black-water tributaries. Floodplain forests in black-water tributaries may exhibit a relatively early tipping point (Flores and others 2024); a percentage of floodplain forest cover loss after which positive feedbacks cause an irreversible shift from a forest-dominated landscape to a landscape consisting of low tree cover ecosystems, such as white-sand savannas or open degraded areas that are maintained by recurrent fire (Flores and others 2016; Flores and others 2017; Flores and Holmgren 2021a). Our study highlights that such a transition is underway. Undoubtedly, this vegetation shift will be associated with tremendous biodiversity loss (for example, Ritter and others 2012; Junk and others 2015; Lugo Carvajal and others 2023) and alter the ecosystem services provided by black-water floodplain forests, including sustaining of commercial and subsistence fisheries (Barthem and Goulding 2007). Furthermore, increasingly fire-prone floodplains of black-water rivers can facilitate the spillover of fire into surrounding forests, affecting the resilience of the wider Amazon forest system at much larger spatial scales than the floodplains themselves. An important conservation priority in the Amazon basin is, therefore, to monitor fires, especially in black-water floodplains. Preventing forest fires in black-water floodplains is likely needed to avoid pervasive vegetation shifts in the near future (Flores and Holmgren 2021a; Flores and others 2024). Such measures could include promoting alternatives for fire-based agricultural practices, in particular in drought years, as well as an expansion of Protected Areas and Indigenous Territories to include floodplains, which are now often not included in such protected areas. In addition, the development of Integrated Fire Management programs by Amazonian countries should recognize the higher flammability and sensitivity of these floodplain ecosystems.

DATA AVAILABILITY

All datasets used in this study are publicly available (see method section). Data derived from MODIS Burned Area Product (Figures 1B, 2, and 3B) and LandSat images (Figure 3C) are included in the supplementary materials.

Declarations

Conflict of interest The authors declare no competing interests.

REFERENCES

Abell R, Thieme ML, Revenga C, Bryer M, Kottelat M, Bogutskaya N, Coad B, Mandrak N, Balderas SC, Bussing W, Stiassny MLJ, Skelton P, Allen GR, Unmack P, Naseka A, Ng R, Sindorf N, Robertson J, Armijo E, Higgins JV, Heibel TJ, Wikramanayake E, Olson D, López HL, Reis RE, Lundberg JG, Sabaj Pérez MH, Petry P. 2008. Freshwater ecoregions of the world: a new map of biogeographic units for freshwater biodiversity conservation. BioScience 58:403–414.

Alencar A, Asner GP, Knapp D, Zarin D. 2011. Temporal variability of forest fires in eastern Amazonia. Ecol Appl 21:2397–2412.

Alencar AA, Brando PM, Asner GP, Putz FE. 2015. Landscape fragmentation, severe drought, and the new amazon forest fire regime. Ecol Appl 25:1493–1505.

Almeida DRAD, Nelson BW, Schietti J, Gorgens EB, Resende AF, Stark SC, Valbuena R. 2016. Contrasting fire damage and fire susceptibility between seasonally flooded forest and upland forest in the central amazon using portable profiling LiDAR. Remote Sens Environ 184:153–160.

Aragão LEOC, Anderson LO, Fonseca MG, Rosan TM, Vedovato LB, Wagner FH, Silva CVJ, Silva Junior CHL, Arai E, Aguiar AP, Barlow J, Berenguer E, Deeter MN, Domingues LG, Gatti L, Gloor M, Malhi Y, Marengo JA, Miller JB, Phillips OL, Saatchi S. 2018. 21st Century drought-related fires counteract the decline of amazon deforestation carbon emissions. Nat Commun 9:536.

Barichivich J, Gloor E, Peylin P, Brienen RJW, Schongart J, Espinoza JC, Pattnayak KC. 2018. Recent intensification of amazon flooding extremes driven by strengthened Walker circulation. Sci Adv 4:2375–2548.

Barlow J, Peres CA. 2008. Fire-mediated dieback and compositional cascade in an Amazonian forest. Philos Trans R Soc B: Biol Sci 363:1787–1794.

Barthem R, Goulding M. 2007. An unexpected ecosystem: the amazon as revealed by fisheries. Amazon conservation association. St. Louis: Missouri Botanical Garden Press.

Berenguer E, Lennox GD, Ferreira J, Malhi Y, Aragão LEOC, Barreto JR, Del Bon Espírito-Santo F, Figueiredo AES, França F, Gardner TA, Joly CA, Palmeira AF, Quesada CA, Rossi LC, de Seixas MMM, Smith CC, Withey K, Barlow J. 2021. Tracking the impacts of El Niño drought and fire in human-modified Amazonian forests. Proc Natl Acad Sci 118:e2019377118.

Carvalho TC, Wittmann F, Piedade MTF, de Resende AF, Silva TSF, Schongart J. 2021. Fires in Amazonian blackwater floodplain forests: Causes, human dimension, and implications for conservation. Front Forests Glob Change 4:755441.

Cochrane MA, Barber CP. 2009. Climate change, human land use and future fires in the Amazon. Global Change Biol 15:601–612.

Congedo L. 2021. Semi-automatic classification plugin: a python tool for the download and processing of remote sensing images in QGIS. J Open Source Softw 6:3172.

Danielson JJ, and Gesch DB. 2011. Global multi-resolution terrain elevation data 2010 (GMTED2010).*in* U. S. G. S. O.-F. R. 2011–1073, editor.

de Resende AF, Nelson BW, Flores BM, de Almeida DR. 2014. Fire damage in seasonally flooded and upland forests of the central amazon. Biotropica 46:643–646.

Decuyper M, Chávez RO, Lohbeck M, Lastra JA, Tsendbazar N, Hackländer J, Herold M, Vågen Tor-G. 2022. Continuous monitoring of forest change dynamics with satellite time series. Remote Sens Environ 269:112829. https://doi.org/10.1016/j.rse.2021.112829.

DeVries B, Decuyper M, Verbesselt J, Zeileis A, Herold M, Joseph S. 2015. Tracking disturbance-regrowth dynamics in tropical forests using structural change detection and Landsat time series. Remote Sens Environ 169:320–334.

dos Santos AR, Nelson BW. 2013. Leaf decomposition and fine fuels in floodplain forests of the Rio Negro in the Brazilian Amazon. J Trop Ecol 29:455–458.

dos Reis M, Graça PMLDA, Yanai AM, Ramos CJP, Fearnside PM. 2021. Forest fires and deforestation in the central amazon: effects of landscape and climate on spatial and temporal dynamics. J Environ Manag 288:112310.

Feldpausch TR, Carvalho L, Macario KD, Ascough PL, Flores CF, Coronado ENH, Kalamandeen M, Phillips OL, Staff RA. 2022. Forest fire history in Amazonia inferred from intensive soil charcoal sampling and radiocarbon dating. Front Forests Globl Change 05:14.

Flores BM, Holmgren M. 2021a. White-sand savannas expand at the core of the amazon after forest wildfires. Ecosystems 24:1624–1637.

Flores BM, Holmgren M. 2021b. Why forest fails to recover after repeated wildfires in Amazonian floodplains? Experimental evidence on tree recruitment limitation. J Ecol 109:3473–3486.

Flores BM, Piedade MTF, Nelson BW. 2014. Fire disturbance in Amazonian blackwater floodplain forests. Plant Ecol Divers 7:319–327.

Flores BM, Fagoaga R, Nelson BW, Holmgren M. 2016. Repeated fires trap Amazonian blackwater floodplains in an open vegetation state. J Appl Ecol 53:1597–1603.

Flores BM, Holmgren M, Xu C, Nes EH, Jakovac CC, Mesquita RCG, Scheffer M. 2017. Floodplains as an Achilles' heel of Amazonian forest resilience. Proc Natl Acad Sci United States Am 114:4442–4446.

Flores BM, Montoya E, Sakschewski B, Nascimento N, Staal A, Betts RA, Levis C, Lapola DM, Esquível-Muelbert A, Jakovac C, Nobre CA, Oliveira RS, Borma LS, Nian D, Boers N, Hecht SB, ter Steege H, Arieira J, Lucas IL, Berenguer E, Marengo JA, Gatti LV, Mattos CRC, Hirota M. 2024. Critical transitions in the amazon forest system. Nature 626:555–564.

Fonseca MG, Anderson LO, Arai E, Shimabukuro YE, Xaud HAM, Xaud MR, Madani N, Wagner FH, Aragão LEOC. 2017. Climatic and anthropogenic drivers of northern amazon fires during the 2015–2016 El Niño event. Ecol Appl 27:2514–2527.

Furch K. 1984. Water chemistry of the amazon basin: the distribution of chemical elements among freshwaters. In: Sioli H, Ed. The amazon. Limnology and landscape ecology of a mighty tropical river and its basin, . Dordrecht: Springer. pp 167–199.

Giglio L, Boschetti L, Roy DP, Humber ML, Justice CO. 2018. The Collection 6 MODIS burned area mapping algorithm and product. Remote Sens Environ 217:72–85. https://doi.org/10.1016/j.rse.2018.08.005.

Gloor M, Brienen RJW, Galbraith D, Feldpausch TR, Schöngart J, Guyot J-L, Espinoza JC, Lloyd J, Phillips OL. 2013. Intensification of the amazon hydrological cycle over the last two decades. Geophys Res Lett 40:1729–1733.

Goulding M, Barthem R, Ferreira EJG. 2003. Smithsonian atlas of the amazon. Washington: Smithsonian Books.

Gumbricht T, Roman-Cuesta RM, Verchot L, Herold M, Wittmann F, Householder E, Herold N, Murdiyarso D. 2017. An expert system model for mapping tropical wetlands and peatlands reveals South America as the largest contributor. Glob Change Biol 23:3581–3599.

Hess LL, Melack JM, Affonso AG, Barbosa C, Gastil-Buhl M, Novo E. 2015. Wetlands of the lowland amazon basin: extent, vegetative cover, and dual-season inundated area as mapped with jers-1 synthetic aperture radar. Wetlands 35:745–756.

Hijmans R 2023. raster: geographic data analysis and modeling. R package version 3.6–26.

Hoffmann WA, Adasme R, Haridasan M, De Carvalho MT, Geiger EL, Pereira MAB, Gotsch SG, Franco AC. 2009. Tree topkill, not mortality, governs the dynamics of savanna-forest boundaries under frequent fire in central Brazil. Ecology 90:1326–1337.

Holmgren M, Scheffer M, Ezcurra E, Gutiérrez JR, Mohren GMJ. 2001. El Niño effects on the dynamics of terrestrial ecosystems. Trends Ecol Evol 16:89–94.

Householder JE, Wittmann F, Schöngart J, Piedade MTF, Junk WJ, Latrubesse EM, Quaresma AC, Demarchi LO, de Lobo GS, Aguiar DPPD, Assis RL, Lopes A, Parolin P, do Leão Amaral I, Coelho LDS, de Almeida Matos FD, Lima Filho DDA, Salomão RP, Castilho CV, Guevara-Andino JE, Carim MDJV, Phillips OL, Cárdenas López D, Magnusson WE, Sabatier D, Revilla JDC, Molino J-F, Irume MV, Martins MP, Guimarães JRDS, Ramos JF, Rodrigues DDJ, Bánki OS, Peres CA, Pitman NCA, Hawes JE, Almeida EJ, Barbosa LF, Cavalheiro L, dos Santos MCV, Luize BG, Novo EMMDL, Núñez Vargas P, Silva TSF, Venticinque EM, Manzatto AG, Reis NFC, Terborgh J, Casula KR, Costa FRC, Honorio Coronado EN, Monteagudo Mendoza A, Montero JC, Feldpausch TR, Aymard GAC, Baraloto C, Castaño Arboleda N, Engel J, Petronelli P, Zartman CE, Killeen TJ, Rincón LM, Marimon BS, Marimon-Junior BH, Schietti J, Sousa TR, Vasquez R, Mostacedo B, do Dantas AD, Castellanos H, Medeiros MBD, Simon MF, Andrade A, Camargo JL, Laurance WF, Laurance SGW, Farias EDS, Lopes MA, Magalhães JLL, Mendonça Nascimento HE, Queiroz HLD, Brienen R, Stevenson PR, Araujo-Murakami A, Baker TR, Cintra BBL, Feitosa YO, Mogollón HF, Noronha JC, Barbosa FR, de Sá CR, Duivenvoorden JF, Silman MR, Ferreira LV, Levis C, Lozada JR, Comiskey JA, Draper FC, Toledo JJD, Damasco G, Dávila N, García-Villacorta R, Vicentini A, Cornejo Valverde F, Alonso A, Arroyo L, Dallmeier F, Gomes VHF, Jimenez EM, Neill D, Peñuela Mora MC, Carvalho FA, Coelho de Souza F, Feeley KJ, Gribel R, Pansonato MP, Ríos Paredes M, Barlow J, Berenguer E, Dexter KG, Ferreira J, Fine PVA, Guedes MC, Huamantupa-Chuquimaco I, Licona JC, Pennington T, Villa Zegarra BE, Vos VA, Cerón C, Fonty É, Henkel TW, Maas P, Pos E, Silveira M, Stropp J, Thomas R, Daly D, Milliken W, Pardo Molina G, Vieira ICG, Albuquerque BW, Campelo W, Emilio T, Fuentes A, Klitgaard B, Marcelo Pena JL, Souza PF, Tello JS, Vriesendorp C, Chave J, Di Fiore A, Hilário RR, Pereira LDO, Phillips JF, Rivas-Torres G, van Andel TR, von Hildebrand P, Balee W, Barbosa EM, Bonates LCDM, Doza HPD, Gómez RZ, Gonzales T, Gonzales GPG, Hoffman B, Junqueira AB, Malhi Y, Miranda IPDA, Mozombite-Pinto LF, Prieto A, Rudas A, Ruschel AR, Silva N, Vela CIA, Zent S, Zent EL, Cano A, Carrero Márquez YA, Correa DF, Costa JBP, Flores BM, Galbraith D, Holmgren M, Kalamandeen M, Nascimento MT, Oliveira AA, Ramirez-Angulo H, Rocha M, Scudeller VV, Sierra R, Tirado M, Umaña MN, van der Heijden G, Vilanova Torre E, Ahuite Reategui MA, Baider C, Balslev H, Cárdenas S, Casas LF, Farfan-Rios W, Ferreira C, Linares-Palomino R, Mendoza C, Mesones I, Parada GA, Torres-Lezama A, Urrego Giraldo LE, Villarroel D, Zagt R, Alexiades MN, de Oliveira EA, Garcia-Cabrera K, Hernandez L, Palacios Cuenca W, Pansini S, Pauletto D, Ramirez Arevalo F, Sampaio AF, Valderrama Sandoval EH, Valenzuela Gamarra L, ter Steege H. 2024. One sixth of Amazonian tree diversity is dependent on river floodplains. Nat Ecol Evol 8:901–911.

Hufkens K 2023. The MODISTools package: an interface to the MODIS Land Products Subsets Web Services.

Jones PD, Lister DH, Osborn TJ, Harpham C, Salmon M, Morice CP. 2012. Hemispheric and large-scale land surface air temperature variations: an extensive revision and an update to 2010. J. Geophys. Res. 117:D05127.

Junk WJ, Piedade MTF, Schongart J, Cohn-Haft M, Adeney JM, Wittmann F. 2011. A classification of major naturally-occurring amazonian lowland wetlands. Wetlands 31:623–640.

Junk WJ, Piedade MTF, Schöngart J, Wittmann F. 2012. A classification of major natural habitats of Amazonian white-water river floodplains (várzeas). Wetlands Ecol Manag 20:461–475.

Junk WJ, Wittmann F, Schongart J, Piedade MTF. 2015. A classification of the major habitats of Amazonian black-water river floodplains and a comparison with their white-water counterparts. Wetlands Ecol Manag 23:677–693.

Kennedy CM, Oakleaf JR, Theobald DM, Baruch-Mordo S, and Kiesecker J 2020. Global human modification of terrestrial systems.*in* N. S. D. a. A. C. S. A. N. 2021, editor., Palisades, NY.

Landerer FW, Swenson SC. 2012. Accuracy of scaled GRACE terrestrial water storage estimates. Water Resour Res 48:1–11.

Landerer F 2021. TELLUS_GRAC_L3_CSR_RL06_LND_v04. Ver. RL06 v04. PO.DAAC, CA, USA. Dataset accessed [2020-01-01] at https://doi.org/10.5067/TELND-3AC64.

Latrubesse EM, Franzinelli E. 2005. The late Quaternary evolution of the Negro River, Amazon, Brazil: Implications for island and floodplain formation in large anabranching tropical systems. Geomorphology 70:372–397.

Lugo Carvajal A, Holmgren M, Zuanon J, van der Sleen P. 2023. Fish on fire: shifts in Amazonian fish communities after floodplain forest fires. J Appl Ecol 60:1637–1646.

Malhi Y, Roberts JT, Betts RA, Killeen TJ, Li WH, Nobre CA. 2008. Climate change, deforestation, and the fate of the Amazon. Science 319:169–172.

Marengo JA, Nobre CA, Tomasella J, Cardoso MF, Oyama MD. 2008. Hydro-climatic and ecological behaviour of the drought of Amazonia in 2005. Philos Trans R S B: Biol Sci 363:1773–1778.

Oliveras I, Malhi Y. 2016. Many shades of green: The dynamic tropical forest–savannah transition zones. Philos Trans R Soc b: Biol Sci 371(1703):20150308. https://doi.org/10.1098/rstb.2015.0308.

Poggio L, de Sousa LM, Batjes NH, Heuvelink GBM, Kempen B, Ribeiro E, Rossiter D. 2021. SoilGrids 2.0: producing soil information for the globe with quantified spatial uncertainty. SOIL 7:217–240.

Rayner NA, Parker DE, Horton EB, Folland CK, Alexander LV, Rowell DP, Kent EC, Kaplan A. 2003. Global analyses of sea surface temperature, sea ice, and night marine air temperature since the late nineteenth century. J Geophys Res d: Atmos. https://doi.org/10.1029/2002JD002670.

Resende AF, Piedade MTF, Feitosa YO, Andrade VHF, Trumbore SE, Durgante FM, Macedo MO, Schongart J. 2020. Flood-pulse disturbances as a threat for long-living Amazonian trees. New Phytol 227:1790–1803.

Ritter CD, Andretti CB, Nelson BW. 2012. Impact of past forest fires on bird populations in flooded forests of the Cuini river in the lowland Amazon. Biotropica 4:449–453.

Rodriguez DRO, et al. 2023. Climate variability of the southern Amazon inferred by a multi-proxy tree-ring approach using *Cedrela fissilis* Vell. Sci Total Environ 871:162064. https://doi.org/10.1016/j.scitotenv.2023.162064.

Sanford RL, Saldarriaga J, Clark KE, Uhl C, Herrera R. 1985. Amazon rainforest fires. Science 227:53–55.

Schöngart J, Piedade MTF, Wittmann F, Junk WJ, Worbes M. 2005. Wood growth patterns of *Macrolobium acaciifolium* (Benth.) Benth. (*Fabaceae*) in Amazonian black-water and white-water floodplain forests. Oecologia 145:454–461.

Silveira MVF, Petri CA, Broggio IS, Chagas GO, Macul MS, Leite CCSS, Ferrari EMM, Amim CGV, Freitas ALR, Motta AZV, Carvalho LME, Silva Junior CHL, Anderson LO, Aragão LEOC. 2020. Drivers of fire anomalies in the Brazilian Amazon: lessons learned from the 2019 fire crisis. Land 9:1–24.

Tapley BD, Bettadpur S, Ries JC, Thompson PF, Watkins MM. 2004. GRACE measurements of mass variability in the earth system. Science 305:503–505.

Venticinque E, Forsberg B, Barthem R, Petry P, Hess L, Mercado A, Canas C, Montoya M, Durigan C, Goulding M. 2016. An explicit GIS-based river basin framework for aquatic ecosystem conservation in the Amazon. Earth Syst Sci Data 8:651–661.

Wittmann F, Schöngart J, Montero JC, Motzer T, Junk WJ, Piedade MTF, Queiroz HL, Worbes M. 2006. Tree species composition and diversity gradients in white-water forests across the amazon basin. J Biogeogr 33:1334–1347.